

Search for Antimatter with the AMS Cosmic Ray Detector

Markus Cristinziani^{a*}

^aD.P.N.C., Université de Genève, CH-1211 Genève 4, Switzerland

Now at: *Stanford Linear Accelerator Center, Stanford, CA 94309, USA*

Antimatter search results of the Alpha Magnetic Spectrometer (AMS) detector are presented. About 10^8 triggers were collected in the 1998 precursor flight onboard space shuttle *Discovery*. This ten day mission exposed the detector on a 51.7° orbit at an altitude around 350km. Identification of charged cosmic rays is achieved by multiple energy loss and time-of-flight measurements. Bending inside the 0.15T magnetic volume yields a measurement of the absolute value of the particle's rigidity. The supplemental knowledge of the sense of traversal identifies the sign of the charge. In the rigidity range $1 < R < 140$ GV no antinucleus at any rigidity was detected, while 2.86×10^6 helium and 1.65×10^5 heavy nuclei were precisely measured. Hence, upper limits on the flux ratio \bar{Z}/Z are given. Different prior assumptions on the antimatter spectrum are considered and corresponding limits are given.

1. Introduction

The Dirac theory of elementary interactions states that to each particle corresponds an antiparticle with all additive quantum numbers inverted in sign, and of each reaction involving particles, the symmetric can occur. An experimental confirmation was provided by the discovery of the positron in cosmic rays [1] and later by the production of antiprotons at accelerators [2]. However we do not observed this symmetry in our macroscopic surrounding which is composed of photons and matter particles. Indeed, there is no undisputed experimental evidence up to now which proves the presence of antimatter in our Universe.

Based on the evidence that in weak interactions parity (P) is not conserved [3] nor is the product of charge conjugation and parity (CP) in the very specific case of the neutral K system [4], Sakharov [5] pointed out that three ingredients are necessary for a baryon symmetric Universe to evolve to an asymmetric one:

- violation of the baryon number (B);
- violation of C and CP ;
- departure from thermal equilibrium.

There is no compelling reason for the baryon number to be strictly conserved and there is no evidence of a force associated with baryonic charge. In fact, GUT theories predict B violating interactions. There are several experiments which are testing B nonconservation by searching for neutron-antineutron oscillations or proton decays, none of them having detected a significant signal so far. The present world limit on the proton lifetime, determined by the partial width of the decay $p \rightarrow e^+ \pi$, is $\tau_p > 1.6 \times 10^{33}$ yrs [6]. The strength of the observed CP violation is far too small to account for the baryon asymmetry of the Universe.

Antimatter does not exist on Earth in macroscopic amounts: it would have been annihilated releasing tremendous amounts of energy. The solar wind, the constant flux of charged particles emitted by the Sun and propagated throughout the solar system, allows us to exclude antimatter planets, which otherwise would appear as very bright γ -ray emitters. Photons emitted by other stars do not probe directly the sign of the baryon number of the object they are emitted from. Fortunately cosmic rays do and we can therefore expect to learn about the baryon content of the Galaxy and the Universe by studying their composition.

*markus@slac.stanford.edu

2. Summary of previous measurements

Balloon-borne experiments started to search for signatures of antinuclei in their instruments since 40 years. A summary of the most stringent limits on the antihelium flux as a function of the observed rigidity range can be found in reference [7]. The BESS collaboration deploy their detector, whose central part is made out of a drift chamber enclosed by a thin superconducting magnet, on balloon flights from a high latitude location on an annual basis since 1993. The latest limit on the antihelium-to-helium flux ratio reported by the BESS collaboration is 7×10^{-7} [8] up to a maximum rigidity of 14 GV.

A comprehensive compilation of limits on the antimatter-to-matter flux ratio is shown in fig. 1.

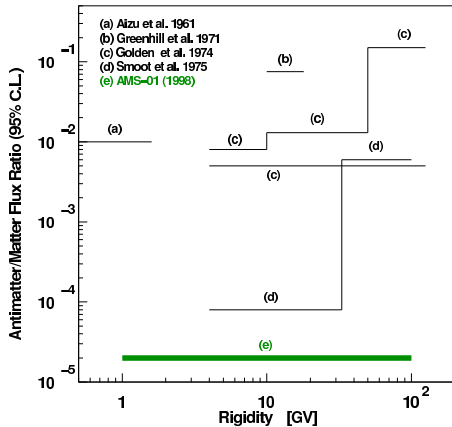


Figure 1. *Compilation of limits on the antimatter-to-matter flux ratio. The AMS-01 measurement provides an improvement both in sensitivity and in rigidity range.*

A stack of photographic emulsions was used in 1961 [9] to detect annihilation topologies with a maximum detectable energy of $E_{\max} = 700$ MeV/n. Greenhill and collaborators [10] employed a gas Čerenkov detector and scintillators for the $|\beta|$ and dE/dx determination in 1971. The traversal direction could not be directly measured but was derived by considerations on the differ-

ent dependence of the cutoff rigidity for negative and positive charged particles for a given orientation of the instrument with respect to zenith. Because of the higher Čerenkov threshold it was possible to exclude the presence of antimatter up to energy values of $E = 9$ GeV/n. The first magnetic spectrograph with spark chambers and emulsion plates recorded a relatively small amount of events, while Golden et al. in 1974 [11] and Smoot et al. in 1975 [12] used a superconducting magnet with a bending power of $BL = 0.43$ Tm. With an acceptance of 0.066 m²sr a total of $\sim 10^4$ events were collected up to rigidity values of $R = 100$ GV. This measurement yielded the most stringent limit for the presence of antinuclei ($Z < -2$) before AMS.

3. The AMS apparatus

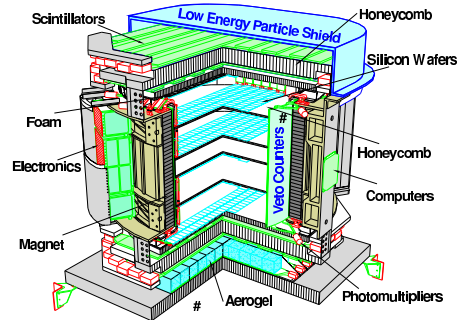


Figure 2. *The AMS-01 detector as flown on space shuttle Discovery in 1998.*

The Alpha Magnetic Spectrometer (AMS) [13] is scheduled for a high energy physics program on the International Space Station. The primary goal of the AMS experiment is the search for antimatter in cosmic rays. The unambiguous signature which is looked for are nuclei with $|Z| > 1$. The physical quantities which are measured by the AMS detector include the particle charge and mass for its identification, its energy or equivalently its rigidity, and the sense and direction of traversal.

The AMS-01 [14] version of the Alpha Magnetic Spectrometer is schematically shown in fig. 2. It was flown on the space shuttle *Discovery* on flight STS-91 in June 1998 for a ten days test flight. The cylindrical permanent magnet encloses a multilayer silicon tracker which measures the trajectory of charged particles traversing the volume. Four scintillator planes and an Aerogel Threshold Čerenkov counter complete the detector by measuring the particle velocity. The energy loss is recorded by the tracker and the scintillators. In order to reject particles outside the magnet aperture the inner wall of the magnet is covered by an anticoincidence counter. To minimize dead time a “Low Energy Particle Shield” absorbs low energy particles above the scintillator planes. For particles arriving from above, the amount of material at normal incidence was 1.5 g/cm^2 in front of the TOF system, and 3.5 g/cm^2 in front of the tracker.

4. Search for antinuclei

A detailed description of the search for anti-helium is given in reference [15].

The goal of the analysis is to find a small amount of antimatter in a large background of matter. A total of 270905 events are identified as particles traversing the detector with $|Z| > 2$, out of which about 6% are initially reconstructed as antimatter candidates:

- Number of events with $Z > 2$: 255321
- Number of events with $Z < -2$: 15584.

In fig. 3 rigidity distributions are shown before and after all selection cuts. The measured parameter is the track’s sagitta, i.e. the deflection, which is proportional to the inverse rigidity $1/R$. The candidate antimatter events are uniformly distributed as a function of $1/R$, which immediately suggests that they predominantly arise from misreconstruction. The event selected with the lowest rigidity has a value $1/R = 1.59 \text{ GV}^{-1}$ or $R = 630 \text{ MV}$. At lower values a background level of ~ 100 events/bin is reached.

A matter nucleus may in principle mimic an antimatter nucleus flying in opposite direction if the time-of-flight is determined with the wrong

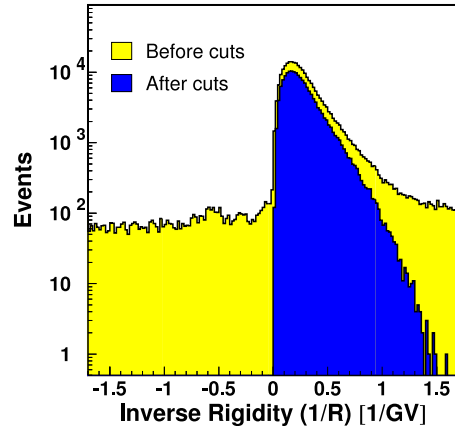


Figure 3. *Event distribution as a function of the inverse rigidity. The event quality cuts remove all $R < 0$ candidates.*

sign. Due to the good time resolution of the TOF system the β measurement is sufficiently accurate not to mix the two particle populations coming from the top and from the bottom of the detector. A misidentification is therefore excluded.

The dynamic range of the silicon tracker allows a good separation of nuclei at least up to oxygen ($Z = 8$). Up to six measurements are available for the same particle. The energy lost inside each silicon detector is measured twice (“S” and “K” side). Fig. 4 shows the obtained separation capability.

A set of cuts has been developed [16] to ensure the selection of clean events. Special care has to be taken to eliminate events which have a poor determination of the track parameters. For example, the rigidity estimations obtained using the upper and lower three tracking points are required to agree.

The last cut is applied to ensure the overall consistence of the velocity, rigidity and charge measurements. Fig. 5 shows the distribution of $1/\beta$ versus rigidity together with the cuts applied for $|Z| > 2$ events. True $|Z| > 2$ events should be concentrated along the line $1/\beta = \sqrt{1 + (AM_n/ZR)^2}$, where A is the atomic number and M_n the nucleon mass. Measurement errors in β , Z or R cause scattering around this line.

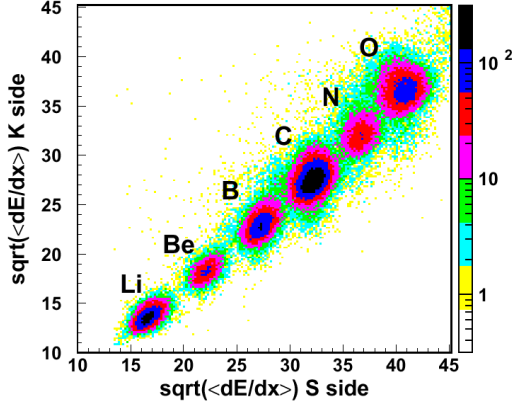


Figure 4. Combined charge measurement by energy loss recorded for S side and K side clusters. Peaks are represented on a logarithmic scale.

The shown cuts reject all remaining $Z < -2$ antimatter candidates and keep nearly all the $Z > 2$ events.

Corrections to the measured spectrum take into account the rigidity resolution function, the detector livetime and rigidity cutoff dependence on the latitude, and the different cross section of nuclei and antinuclei hitting the detector material.

5. Limits on the antimatter-to-matter flux ratio

Since no antimatter nucleus was found at any rigidity, one can provide an upper limit on the flux ratio of antimatter to matter $N_{\bar{Z}}/N_Z$ which is evaluated by summing up the contents of all the bins

$$\left[\frac{N_{\bar{Z}}}{N_Z} \right] = \frac{\sum N_{\bar{Z}}(R_i)}{\sum N_Z(R_i)}.$$

It should be noted that the experimental result of detecting no antimatter nucleus corresponds to $\sum N'_{\bar{Z}}(R_i) = 0$, where N' denotes the *measured* spectrum.

Following the unified approach of confidence belts construction proposed in [17] which ensures correct coverage avoiding unphysical confidence intervals and is based on classical statistics, we can put $\sum N'_{\bar{Z}}(R_i) < 3.09$ at a 95% confidence

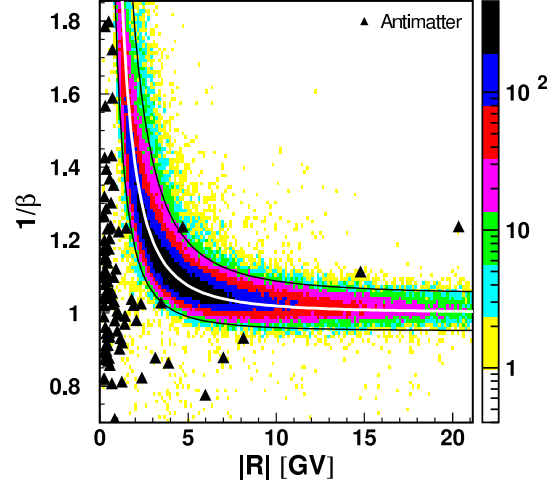


Figure 5. Time-of-flight vs. absolute rigidity [18]. Nuclei with $(mc^2/Ze)^2 \sim 4 \text{ GV}^2$ should lie along the white line. Well reconstructed events are selected within the black lines. All the antimatter candidates (triangles) are outside this region.

level.

Three different priors can be assumed for the unknown antimatter distribution, $N_{\bar{Z}}(R_i)$:

- the same spectrum as matter, $N_{\bar{Z}}(R_i)/N_Z(R_i) = \text{const}$;
- a flat spectrum, $N_{\bar{Z}}(R_i) = \text{const}$;
- no a priori spectrum (worst case), $N_{\bar{Z}}(R_j) = N_{\bar{Z}}$, where j is the bin with the lowest efficiency and $N_{\bar{Z}}(R_i) = 0$ otherwise.

Limits for the three approaches are calculated as follows (see reference [7] for details):

$$\left[\frac{N_{\bar{Z}}}{N_Z} \right]_{\text{same}} < \frac{3.09}{\sum N'_Z(R_i) \frac{\epsilon_{\bar{Z}}(R_i)}{\epsilon_Z(R_i)}},$$

$$\left[\frac{N_{\bar{Z}}}{N_Z} \right]_{\text{unif}} < \frac{3.09 / \langle \epsilon_{\bar{Z}} \rangle}{\sum N'_Z(R_i) / \epsilon_Z(R_i)},$$

$$\left[\frac{N_{\bar{Z}}}{N_Z} \right]_{\text{cons}} < \frac{3.09 / \epsilon_{\min}}{\sum N'_Z(R_i) / \epsilon_Z(R_i)}.$$

where $\epsilon_Z(R_i)$ and $\epsilon_{\bar{Z}}(R_i)$ are the detector efficiencies for matter and antimatter, the *average*

efficiency is defined as $\langle \epsilon_{\bar{Z}} \rangle \equiv (\sum \epsilon_Z(R_i))/n$, and ϵ_{\min} is the worst efficiency in a given rigidity interval.

Under the same spectrum assumption $[N_{\bar{Z}}/N_Z]_{\text{same}} < 2.00 \times 10^{-5}$ for all nuclei. This result is compared to previous measurements in fig. 1. A more stringent limit could be given due to the amount of events collected and the good rigidity resolution. The rigidity range extends from 1 GV to 100 GV.

In the second case, the upper limit on the anti-carbon/carbon ratio, for example, is 6.55×10^{-5} in the rigidity range 1GV to 10GV and 1.46×10^{-4} in the range 1 GV to 50 GV.

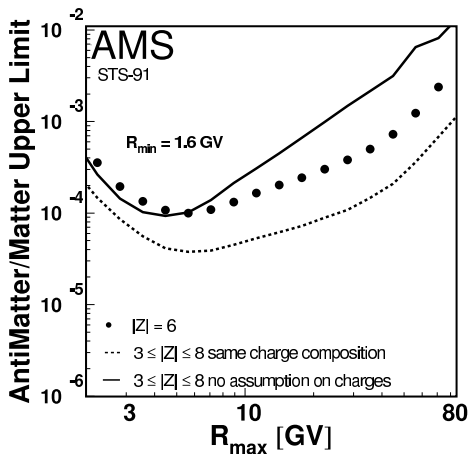


Figure 6. Upper limits on the antimatter-to-matter flux ratio under the conservative approach. Integrating over the rigidity range $[R_{\min} = 1.6 \text{ GV}; R_{\max}]$, the limit curves are shown as a function of the maximal rigidity R_{\max} .

The upper limit determined under the most conservative assumption is shown in fig. 6 for all matter/antimatter nuclei ($3 \leq |Z| \leq 8$) and for carbon/anticarbon. Starting from a minimum rigidity of $R_{\min} = 1.6 \text{ GV}$ the upper limit is shown as a function of the maximum rigidity. With increasing R_{\max} the limits decrease as a consequence of the increasing statistics. The rise above $R_{\max} \sim 4 \text{ GV}$ is due to the detection efficiency

which gets worse with increasing rigidity. The corresponding result for antihelium can be found in [15].

With the AMS-01 test flight a never before obtained sensitivity for antimatter searches has been reached. The AMS-02 version of the detector which will include a superconducting magnet and will be installed on the International Space Station is foreseen to further improve this sensitivity up to TV rigidities [19].

REFERENCES

1. C. D. Anderson, Phys. Rev. 43 (1933) 491
2. O. Chamberlain et al., Phys. Rev. 100 (1955) 947
3. S. Wu et al., Phys. Rev. 105 (1957) 1413
4. J. H. Christenson et al., Phys. Rev. Lett. 13 (1964) 138
5. A. D. Sakharov, Sov. Phys. JETP Lett. 5 (1967) 24
6. K. Hagiwara et al., Phys. Rev. D 66 (2002) 1
7. M. Cristinziani, Proc. 1st Int. Conf. on Particle and Fundamental Physics in Space (La Biodola, Elba), to appear in Nucl. Phys. B, Proc. Suppl.
8. M. Sasaki et al. (BESS), Proc. 27th Int. Cosmic Ray Conf. (Hamburg), 5 (2001) 1711
9. H. Aizu et al., Phys. Rev. 121 (1961) 1206
10. J. G. Greenhill et al., Nature 230 (1971) 170
11. R. L. Golden et al., Astrophys. J. 192 (1974) 747
12. G. F. Smoot et al., Phys. Rev. Lett. 35 (1975) 258
13. S. Ahlen et al., Nucl. Instrum. Meth. A 350 (1994) 351
14. G. M. Viertel and M. Capell, Nucl. Instrum. Meth. A 419 (1998) 295
15. J. Alcaraz et al., Phys. Lett. B 461 (1999) 387
16. M. Cristinziani, PhD thesis, Université de Genève, 2002
17. G. J. Feldman and R. D. Cousins, Phys. Rev. D 57 (1998) 3873
18. M. Cristinziani (AMS), Proc. 27th Int. Cosmic Ray Conf. (Hamburg), 5 (2001) 1703
19. J. Casaus, these proceedings